

Passivity-based control of a wound-rotor synchronous motor

Arnau Dòria-Cerezo^{a*}, Carles Batlle^b, and Gerardo Espinosa-Pérez^c

^a*Department of Electrical Engineering and Institute of Industrial and Control Engineering,
Universitat Politècnica de Catalunya, EPSEVG, 08800 Vilanova i la Geltrú, Spain*

^b*Department of Applied Mathematics IV and Institute of Industrial and Control Engineering,
Universitat Politècnica de Catalunya, EPSEVG, 08800 Vilanova i la Geltrú, Spain*

^c*Facultad de Ingeniería,*

Universidad Nacional Autónoma de México, 04510 México DF, México

Abstract

This paper presents a new nonlinear passivity-based controller for a wound rotor synchronous machine, acting as a motor drive. The control objectives are stated in the dq -frame, and the port-controlled Hamiltonian model is also obtained. A power flow analysis allows to state the control goals in terms of reactive power compensation and ohmic losses reduction. From the Hamiltonian structure, the Simultaneous Interconnection and Damping Assignment (SIDA-PBC) technique is used to compute the control action, which results in a controller with a simpler architecture than the standard one for this class of machines, able to cope with both positive and negative external mechanical loads and having thus bidirectional power capabilities. The robustness of the control action is also taken into account in the design procedure. Finally, the computed controller is validated via numerical simulations.

Keywords: passivity-based control; Simultaneous IDA-PBC; electrical machines; wound rotor synchronous motor

*Corresponding author. Email: arnau.doria@upc.edu

1 Introduction

The wound rotor synchronous machine (WRSM) is used for generation and also for drive applications [1]. In the generation case the field voltage is used to regulate the stator voltage, while for motor applications this variable can be used to compensate the power factor of the machine [2]. Several techniques for the control of the WRSM have been proposed in the literature. Linear techniques are the most used in the industry [3][4], but decoupling methods [5], widely employed for asynchronous machines, have also been extended to the synchronous case, and advanced nonlinear controllers have been applied to this class of machines as well [6][7]. For many applications a bidirectional power flow is required. An example can be found in Hybrid Electrical Vehicles, HEV [8] where the regenerative braking (employed to store kinetic energy into the batteries) is achieved using the electrical machine as a generator, by consigning a negative torque.

The main advantage of using a WRSM in front of the permanent magnet synchronous motor (PMSM), is the ability to compensate the reactive power consumed by the electrical machine. This feature can be done by selecting the appropriate rotor flux using the field voltage.

Usually, synchronous motors are controlled using two control loops. An inner current loop is designed to regulate the dq components of the stator current, and one or more outer loops provide the desired values of current to achieve the control goals (mechanical speed and reactive power). The proof of stability of this scheme is usually performed by invoking a time scale separation between the dynamics of the electrical and mechanical variables. In this paper, using passivity-based techniques, the speed controller is moved into the inner loop, the stability of which is proved rigorously in a passivity-based framework.

Passivity-based control (PBC) is a technique that can be used to design controllers for a large kind of systems. Control of a rather general class of electrical machines using PBC methods has been proposed in [9], and the specific cases for synchronous generators and drives can be found also in [10][11], respectively. Recently, a new technique based on the PBC properties called Interconnection and Damping Assignment (IDA-PBC) has been proposed in [12]. Using the IDA-PBC approach many electrical machines have been controlled [13], in particular induction machines (see example in [14]) and permanent magnet synchronous ones [15]. The simultaneous IDA-PBC methodology was proposed in [16], where the induction machine was studied and controlled. The SIDA-PBC technique offers more degrees of freedom than IDA-PBC, and allows to

solve more complex interconnected systems and to design output feedback, as opposed to state feedback, controllers (see examples in [16] and [17]).

The main goal of this work is to design a control algorithm to regulate a wound rotor synchronous drive machine, based on the Simultaneous IDA-PBC technique. The paper is organized as follows. In Section 3 the wound rotor synchronous machine model is introduced and its control goals are described. Section 4 presents the SIDA-PBC technique and then the control law is obtained. The simulation results are included in Section 5 and, finally, conclusions are stated in Section 6.

Throughout the paper $*$ designs fixed point values while d is used for desired regulation values.

2 SIDA-PBC technique

The Simultaneous Interconnection and Damping Assignment (SIDA-PBC) method was proposed in [16] as a generalization of the Interconnection and Damping Assignment (IDA-PBC) technique [18][12]. It considers the problem of designing an state space controller for the stabilization of a desired equilibrium point of a nonlinear system $\dot{x} = f(x) + g(x)u$.

The key idea behind the SIDA-PBC technique (as it occurs also in the classic IDA-PBC) is to match the closed-loop dynamics to a PCHS form

$$f(x) + g(x)u = F_d(x)\partial H_d, \quad (1)$$

where F_d is a $n \times n$ matrix and $H_d(x) : \mathbb{R}^n \rightarrow \mathbb{R}$, and the ∂_x (or ∂ , if no confusion arises) operator defines the gradient of a function of x , and in what follows we will take it as a column vector. The left hand side of (1) may also be given in explicit PCHS [19][20] form $(J(x) - R(x))\partial H(x) + g(x)u$.

To enforce dissipativity, the following constraint on the F_d matrix is required

$$F_d(x)^T + F_d(x) \leq 0. \quad (2)$$

The equilibrium assignment of the desired energy function translates to

$$x^d = \arg \min H_d(x). \quad (3)$$

In (1) one has $x \in \mathbb{R}^n$ and $u \in \mathbb{R}^m$, with $m \leq n$ and, in practice, $m < n$. Furthermore, the m columns of the $n \times m$ matrix $g(x)$ are assumed to be independent (if they are not one just has an overparametrization of the control input u), which is equivalent to $g^T g$ being invertible. If $m < n$, there is a basis of $n - m$ left vectors of g , which can be arranged row-wise in a matrix g^\perp such that $g^\perp g = 0$. Operating with g^\perp on the left of (1) one gets the so-called matching equation

$$g^\perp(x)f(x) = g^\perp(x)F_d(x)\partial H_d(x), \quad (4)$$

which is either a partial differential equation for H_d [12] with the additional requirement (3) if F_d is given, or an algebraic equation for F_d [21] subjected to (2), if a suitable H_d is provided, or a mix of both (see [22] for a survey). In this paper the algebraic approach will be adopted. With appropriate F_d and H_d choices, the control is obtained from (1) as

$$u = (g(x)^T g(x))^{-1} g^T(x)(F_d(x)\partial H_d(x) - f(x)), \quad (5)$$

where the invertibility of $g^T g$ has been employed. Note that the closed loop system defined by

$$\dot{x} = F_d(x)\partial H_d \quad (6)$$

can be easily written in a PCHS form

$$\dot{x} = (J_d(x) - R_d(x))\partial H_d(x) \quad (7)$$

with

$$J_d(x) = \frac{F_d(x) - F_d(x)^T}{2}, R_d = -\frac{F_d(x) + F_d(x)^T}{2}. \quad (8)$$

3 The WRSM model and control goals

In this section we present the dynamical model of the WRSM. From the well-known dynamical equations we also propose a port-Hamiltonian model which allows to describe in a compact form and with a nice physical interpretation the system dynamics. Although the SIDA-PBC technique does not require to have the model in PCHS form, it can help in the design process. Finally, we compute, in terms of the fixed point values, the active and reactive powers flowing

through the stator side of the machine and define the control objectives.

Figure 1 shows the scheme connection of a wound rotor synchronous machine acting as a motor.

3.1 dq-model of the WRSM

The dq transformation [23] is commonly used to transform a tracking problem into a regulation one. The steady-state for the three phase electrical variables is given by periodic orbits which can be transformed into equilibrium points of a new two phase dq -system.

The state space model in dq coordinates of a wound rotor synchronous machine with a field winding (and no damper windings) is given by [24]

$$\dot{\lambda}_d = -R_s i_d + n_p \omega L_s i_q + v_d \quad (9)$$

$$\dot{\lambda}_q = -n_p \omega L_s i_d - R_s i_q - n_p \omega M i_F + v_q \quad (10)$$

$$\dot{\lambda}_F = -R_F i_F + v_F \quad (11)$$

where $\lambda^T = (\lambda_d, \lambda_q, \lambda_F) \in \mathbb{R}^3$ and $i^T = (i_d, i_q, i_F) \in \mathbb{R}^3$ are the fluxes and currents, respectively¹, ω is the mechanical speed, n_p is the number of pole pairs, R_s and R_F are the ohmic resistances of the stator dq and rotor field windings, and L_s , L_F and M are the leakage and mutual inductances.

The dynamical model has to be completed with the mechanical equation

$$J_m \frac{d\omega}{dt} = n_p M i_F i_q - B_r \omega + \tau_L. \quad (12)$$

Here J_m is the rotor inertia, τ_L is a generic mechanical torque (negative in case of braking), and B_r is a viscous mechanical damping coefficient.

Fluxes and currents are related by $\lambda = Li$ where

$$L = \begin{pmatrix} L_s & 0 & M \\ 0 & L_s & 0 \\ M & 0 & L_F \end{pmatrix}. \quad (13)$$

¹ d , q and F subindexes refers to dq coordinates and the field variables, respectively.

3.2 Port-Hamiltonian model of the WRSM

Port-Hamiltonian modeling uses the state dependent energy functions to characterize the dynamics of the different subsystems, and connects them by means of network relations, such as Kirchhoff's laws in the case of circuit theory or the two source-independent Maxwell equations for electromagnetism, which embody the power preserving physical laws. The result is a mathematical model with an specific structure, called port-controlled Hamiltonian system (PCHS, [25]), which lends itself to a natural, physics-based analysis and control design [26][18].

Explicit PCHS have the form

$$\begin{cases} \dot{x} &= (J(x) - R(x))\partial_x H(x) + g(x)u \\ y &= g^T(x)\partial_x H(x) \end{cases}, \quad (14)$$

where $x \in \mathbb{R}^n$ is the vector state, $u, y \in \mathbb{R}^m$ are the port variables, and $H(x) : \mathbb{R}^n \rightarrow \mathbb{R}$ is the Hamiltonian function, representing the energy function of the system. The ∂_x (or ∂ , if no confusion arises) operator defines the gradient of a function of x , and in what follows we will take it as a column vector. $J(x) \in \mathbb{R}^{n \times n}$ is the interconnection matrix, which is skew-symmetric ($J(x) = -J(x)^T$), representing the internal energy flow in the system, and $R(x) \in \mathbb{R}^{n \times n}$ is the dissipation matrix, symmetric and, in physical systems, semi-positive definite ($R(x) = R^T \geq 0$), which accounts for the internal losses of the system. Finally, $g(x) \in \mathbb{R}^{n \times m}$ is a port matrix describing the port connection of the system to the outside the world. It yields the flow of energy to/from the system through the port variables, u and y .

Equations (9), (10), (11) and (12) can be given a port-Hamiltonian form using as energy variables the fluxes ($\lambda_d, \lambda_q, \lambda_F$) and the momentum ($p = J_m \omega$). Then, the interconnection and dissipation matrices are, respectively

$$J(x) = \begin{pmatrix} 0 & n_p L_s \omega & 0 & 0 \\ -n_p L_s \omega & 0 & 0 & -n_p M i_F \\ 0 & 0 & 0 & 0 \\ 0 & n_p M i_F & 0 & 0 \end{pmatrix}, \quad (15)$$

$$R = \begin{pmatrix} R_s & 0 & 0 & 0 \\ 0 & R_s & 0 & 0 \\ 0 & 0 & R_F & 0 \\ 0 & 0 & 0 & B_r \end{pmatrix}, \quad (16)$$

with Hamiltonian (energy) function

$$H(x) = \frac{1}{2}\lambda^T L^{-1}\lambda + \frac{1}{2J_m}p^2, \quad (17)$$

and with port matrix

$$g = \begin{pmatrix} 1 & 0 & 0 \\ 0 & 1 & 0 \\ 0 & 0 & 1 \\ 0 & 0 & 0 \end{pmatrix}, \quad (18)$$

where the external inputs available for control are $u = (v_d, v_q, v_F)$. The external mechanical torque τ_L will be treated as a perturbation of the model, and hence the PCHS with dissipation and added perturbation to which the SIDA-PBC technique will be applied is

$$\dot{x} = (J - R)\partial H + gu + g_L\tau_L, \quad (19)$$

with $g_L = (0 \ 0 \ 0 \ 1)^T$. The left null vector of g is given by $g^\perp = (0 \ 0 \ 0 \ 1)^T$.

3.3 Fixed points and power flow study

In this subsection we compute, in steady-state, the reactive power flowing through the stator side of the machine (in order to compensate the power factor) and we also establish the power balance of the machine. Throughout this study we consider that the three-phase system is sinusoidal and balanced.

Fixed points are solutions to

$$0 = -R_s i_d^* + n_p \omega^* L_s i_q^* + v_d \quad (20)$$

$$0 = -n_p \omega^* L_s i_d^* - R_s i_q^* - n_p \omega^* M i_F^* + v_q \quad (21)$$

$$0 = -R_F i_F^* + v_F \quad (22)$$

$$0 = n_p M i_F^* i_q^* - B_r \omega^* + \tau_L. \quad (23)$$

In this set of equations, ω^* will be fixed to the desired value ω^d , while the desired values of i_F^* and i_d^* will be computed from additional power and quality requirements. With τ_L considered as an external perturbation, the four equations above can be used to compute i_q^* and the steady state values of v_d , v_q and v_F . In dq -coordinates, the reactive power reads

$$Q_s = v_d i_q - v_q i_d, \quad (24)$$

and using the fixed points (20) and (21), we obtain

$$Q_s^* = -n_p \omega^* (L_s (i_d^{*2} + i_q^{*2}) + M i_d^* i_F^*). \quad (25)$$

Notice that a suitable value of i_F^* can compensate the power factor, *i.e.* $Q_s^* = 0$.

A power balance study is next performed to determine the optimal i_d current in order to minimize the electrical losses P_l . Those can be computed as the difference between the electrical power supplied to the machine (P_s and P_F) and the delivered mechanical power,

$$P_l^* = P_s^* + P_r^* - P_m^*. \quad (26)$$

From the definition of the stator dq -active power,

$$P_s = v_d i_d + v_q i_q, \quad (27)$$

and using the fixed points (20) and (21), we obtain

$$P_s^* = R_s (i_d^{*2} + i_q^{*2}) + n_p \omega^* M i_F^* i_q^*. \quad (28)$$

The rotor power can be easily computed using

$$P_F = v_F i_F \quad (29)$$

which, in steady state and using (22), is rewritten as

$$P_F^* = R_F i_F^{*2}. \quad (30)$$

Finally, the generated mechanical power is defined as the product of the electrical torque and the mechanical speed,

$$P_m^* = \tau_e^* \omega^*. \quad (31)$$

Putting together (28), (30) and (31) in (26) and tacking into account $\tau_e = n_p M i_F i_q$, we recover the electrical losses,

$$P_l = R_s (i_d^{*2} + i_q^{*2}) + R_F i_F^{*2}. \quad (32)$$

Let us introduce the polar coordinates, I and δ , such that

$$i_d^* = I^* \cos \delta^* \quad (33)$$

$$i_q^* = I^* \sin \delta^*. \quad (34)$$

Taking into account (23) and considering that the reactive power goal $Q_s^* = 0$ is achieved, which in polar coordinates is

$$n_p L_s I^{*2} + (B_r \omega^* - \tau_L) \frac{\cos \delta^*}{\sin \delta^*} = 0, \quad (35)$$

equation (32) can be rewritten as

$$P_l = -\frac{(B_r \omega^* - \tau_L)}{n_p} \left(\frac{R_s \cos \delta^*}{L_s \sin \delta^*} + \frac{R_F L_s}{M^2} \frac{1}{\sin \delta^* \cos \delta^*} \right) \quad (36)$$

This function has a minimum at

$$\delta^{op} = \pi - \arccos \left(-\sqrt{\frac{R_F L_s^2}{2R_F L_s^2 + R_s M^2}} \right),$$

which implies, with (35) and (33), that

$$i_d^{op} = I^{op} \cos \delta^{op} \quad (37)$$

where

$$I^{op} = \sqrt{\frac{(B_r \omega^* - \tau_L) \cos \delta^{op}}{n_p L_s \sin \delta^{op}}}. \quad (38)$$

Note that δ^{op} only depends on the electrical parameters, while the mechanical ones B_r and τ_L appear in I^{op} . The latter equation can be rewritten, with the help of (23), as

$$I^{op} = \sqrt{\frac{M}{L_s} i_F^* i_q^* \frac{\cos \delta^{op}}{\sin \delta^{op}}}. \quad (39)$$

3.4 Control objectives

Following the results presented above, we can summarize the control goals as follows: to regulate the mechanical speed at a desired value ω^d , and to compensate the power factor, *i.e.* $Q_s^d = 0$, and also to minimize losses regulating i_d at the optimal point i_d^{op} . To achieve these objectives we have three control inputs, namely v_d , v_q and v_F .

4 Control design

Figure 2 shows the proposed control scheme. As explained above the control objectives are to regulate $\omega^* = \omega^d$, to compensate the reactive power and to regulate i_d at the optimal value in order to minimize losses ($i_d^* = i_d^{op}$). The complete controller consists has an inner-loop which regulates the i_d and i_F current and the mechanical speed, and an outer-loop which computes the required value of i_F to compensate the reactive power.

A passivity-based controller, using the Simultaneous IDA-PBC approach, is designed for the inner-loop. The obtained control law ensures asymptotic stability. This new design also improves the one presented in [27], since there is no restriction on the maximum values of the control gains, and also the control law allows for negative i_F^* values.

The reactive power is regulated with the Q Controller block in Figure 2. The design of this outer-loop is based on the assumption that the inner-loop is much faster than the factor power compensation dynamics. Figure 3 shows the structure of the standard architecture for

this machine [24]. The Speed Controller of the classical architecture has been moved to the SIDA-PBC Controller in our scheme, and instead of the Back-EMF Compensator, the controller is designed in order to minimize the ohmic losses by means of the selection of i_d^{op} , and this has been incorporated also into the SIDA-PBC Controller block.

In this Section, we first present the inner-loop control design, using SIDA-PBC technique, and finally we propose a control law for the power factor compensation.

4.1 SIDA-PBC for the WRSM

As proposed in Section 2, we will use the SIDA-PBC approach to design the inner-control loop for the WRSM. First we fix the energy function as

$$H_d = \frac{1}{2}(x - x^*)^T P(x - x^*) \quad (40)$$

where $x^{*T} = (\lambda_d^*, \lambda_q^*, \lambda_F^*, J_m \omega^*)$ and

$$P = \frac{1}{\mu} \begin{pmatrix} \gamma_d L_F & 0 & -\gamma_d M & 0 \\ 0 & \gamma_q \frac{\mu}{L_s} & 0 & 0 \\ -\gamma_F M & 0 & \gamma_F L_s & 0 \\ 0 & 0 & 0 & \frac{\gamma_\omega}{J_m} \end{pmatrix} \quad (41)$$

with $\mu = L_s L_F - M^2 > 0$. Note that the positiveness requirement on P implies that $\gamma_d = \gamma_F$ and $\gamma_q, \gamma_F, \gamma_\omega > 0$. The main reason for this choice is that it implies to decouple the error in terms of the currents (which are measurables) instead of fluxes, *i.e.*, computing $\partial_x H_d$ and using the inductance matrix (13),

$$\partial_x H_d = \begin{pmatrix} \gamma_F (i_d - i_d^{op}) \\ \gamma_q (i_q - i_q^*) \\ \gamma_F (i_F - i_F^d) \\ \gamma_\omega (\omega - \omega^d) \end{pmatrix}. \quad (42)$$

The $F_d(x)$ matrix is chosen in order to facilitate the solution of the resulting algebraic equations. Furthermore, in order to simplify the control structure, we want to assign one output to each control action and also to obtain a controller as simpler and robust (minimum parameter

dependence) as possible. The proposed structure is as follows

$$F_d(x) = \begin{pmatrix} F_{11}(x) & 0 & 0 & 0 \\ 0 & 0 & 0 & F_{24}(x) \\ 0 & 0 & F_{33}(x) & 0 \\ 0 & F_{42}(x) & F_{43}(x) & F_{44}(x) \end{pmatrix}, \quad (43)$$

which must also satisfy the inequality (2).

Decoupling control actions and feedback outputs is possible if the $F_d(x)$ matrix contains only one nonzero element in each row. The three first rows of $F_d(x)$ have nonzero F_{11} , F_{24} and F_{33} elements, which relate v_d , v_q and v_F to the errors in i_d , ω and i_F , respectively.

Acting with g^T on (19), which selects the three first rows, one obtains the control actions

$$v_d = R_s i_d - n_p \omega L_s i_q + F_{11} \gamma_F (i_d - i_d^{op}) \quad (44)$$

$$v_q = n_p \omega L_s i_d + R_s i_q + n_p \omega M i_F + F_{24} \gamma_\omega (\omega - \omega^d) \quad (45)$$

$$v_F = R_F i_F + F_{33} \gamma_F (i_F - i_F^d), \quad (46)$$

while operating with g^\perp , which in this case singles out the fourth row, one gets the matching equation

$$n_p M i_F i_q - B_r \omega + \tau_L - F_{42} \gamma_q (i_q - i_q^*) - F_{43} \gamma_F (i_F - i_F^d) - F_{44} \gamma_\omega (\omega - \omega^d) = 0. \quad (47)$$

Equation (47) can be solved with

$$F_{42} = \frac{1}{\gamma_q} n_p M i_F^d \quad (48)$$

$$F_{43} = \frac{1}{\gamma_F} n_p M i_q \quad (49)$$

$$F_{44} = -\frac{1}{\gamma_\omega} B_r \quad (50)$$

where the steady-state solution of (12)

$$\tau_L = -n_p M i_F^d i_q^* + B_r \omega^d \quad (51)$$

has been also used. This means that we assume that the dynamics of i_q is much faster than the characteristic time of variation of the external load torque; notice however that we are not supposing anything with respect to the characteristic time of the mechanical variable ω .

In order to simplify the solution, now we assign

$$F_{24} = -F_{42}. \quad (52)$$

With this choice, it is clear that (2) holds if $F_{11}, F_{33} < 0$ and

$$4F_{33}F_{44} - F_{43}^2 > 0 \quad (53)$$

or substituting,

$$-4F_{33} \frac{B_r}{\gamma_\omega} - \left(\frac{1}{\gamma_F} n_p M i_q \right)^2 > 0. \quad (54)$$

Finally, with

$$F_{33} = -\frac{1}{4} n_p^2 M^2 i_q^2 \leq 0 \quad (55)$$

the previous equation reduces to

$$\gamma_\omega < B_r \gamma_F^2. \quad (56)$$

To further simplify the controller the following parameters are assigned

$$F_{11} = -\frac{k_d}{\gamma_F} \quad (57)$$

$$\gamma_q = \frac{16}{n_p^3 M^3} \frac{k_F^2}{k_\omega} \epsilon, \quad (58)$$

$$\gamma_F = \frac{4}{n_p^2 M^2} k_F, \quad (59)$$

$$\gamma_\omega = \frac{\gamma_q}{n_p M} k_\omega, \quad (60)$$

where $\epsilon > 0$ is a remaining free design parameter. With this the controller becomes

$$v_d = R_s i_d - n_p \omega L_s i_q - k_d (i_d - i_d^{op}), \quad (61)$$

$$v_q = n_p \omega L_s i_d + R_s i_q + n_p \omega M i_F - i_F^d k_\omega (\omega - \omega^*), \quad (62)$$

$$v_F = R_F i_F - k_F i_q^2 (i_F - i_F^d), \quad (63)$$

while the stability condition (56) simplifies to $\epsilon < B_r$. However, ϵ does not appear in the control gain ranges, and so it is not even necessary to know a lower bound for B_r in order to implement the above controller. The condition on ϵ is hence only necessary to prove stability, and it relies on $B_r > 0$, which is a sensible assumption for any real machine. With this, stability of the inner-loop is ensured for any $k_d, k_F, k_\omega > 0$ values. Notice that the stability of this inner loop is what in the literature is discussed in terms of the time-scale separation of electrical and mechanical dynamics, and that one of the main contributions of the present paper is to solve this question using a single, more rigorous step.

The controller (61)(62)(63) contains a part that looks like a classic feedback linearization, but the field control action v_F introduces a nonlinear term $k_F i_q^2 (i_F - i_F^d)$.

4.2 Reactive power control loop

As mentioned above, the power factor is compensated via the field current i_F , see equation (25). The proposed control law to achieve the power factor compensations consists in

$$i_F^d = \frac{k_i}{i_d^{op} \omega^d} \int (Q_s - Q_s^d) dt. \quad (64)$$

An argument can be given for the stability of the complete closed-loop system from the fact that the inner loop is faster than the Q_s outer loop. Then, considering that the i_d, i_q, i_F and ω reaches its desired values $(i_d^{op}, i_q^*, i_F^d, \omega^d)$, from (24) the Q_s dynamics yields

$$\dot{Q}_s = -n_p M \omega^d i_d^{op} \frac{di_F^d}{dt}. \quad (65)$$

Finally, the closed loop dynamics is obtained replacing (64),

$$\dot{Q}_s = -k_i n_p M (Q_s - Q_s^d), \quad (66)$$

which clearly stabilizes at $Q_s = Q_s^d$.

In order to find a range of values for k_i for which the stability of the whole system is ensured, let us to consider the extended system $z_e^T = (x^T, z)$, where $z = i_F^d$. Then the whole system is composed by the closed loop system designed in the previous subsection and the designed

dynamics for z , given by (64), *i.e.*

$$\dot{z} = \frac{k_i}{i_d^{op} \omega^d} (Q_s - Q_s^d). \quad (67)$$

Taking as a Lyapunov new function $H_{dz}(z_e)$,

$$H_{dz}(z_e) = H_d(x, z) \geq 0 \quad (68)$$

where i_F^d has been replaced by z , its derivative yields

$$\dot{H}_{dz} = (\partial_x H_d)^T \dot{x} + (\partial_z H_d)^T \dot{z}. \quad (69)$$

Computing the $\partial_z H_d$ term, and replacing the x and z dynamics,

$$\dot{H}_{dz} = (\partial_x H_d)^T F_d \partial_x H_d - \gamma_F (i_F - z) \frac{k_i}{i_d^{op} \omega^d} (Q_s - Q_s^d). \quad (70)$$

Using (42) and (43), the latter results in

$$\dot{H}_{dz} = -k_d \gamma_F (i_d - i_d^{op})^2 - h(x)^T D h(x) + \frac{k_i}{i_d^{op} \omega^d} h(x)^T b(x), \quad (71)$$

where $h(x)^T = (\gamma_F (i_F - z), \gamma_\omega (\omega - \omega^d))$, $b(x)^T = (-(Q_s - Q_s^d), 0)$ and

$$D = - \begin{pmatrix} F_{11} & \frac{1}{2} F_{43} \\ \frac{1}{2} F_{43} & F_{44} \end{pmatrix}, \quad (72)$$

which, from the design in the previous subsection, $D = D^T \geq 0$.

At this point, inspired by Lemma 9.2 in [28], and assuming that $b(x)$ can be bounded, $\|b(x)\| < \delta$, defining $\lambda_{\min} \geq 0$ as the minimum eigenvalue of D and $\theta < 1$ is some positive constant, the time derivative of $H_{dz}(z_e)$ satisfies

$$\dot{H}_{dz} \leq -k_d \gamma_F (i_d - i_d^{op})^2 - \lambda_{\min} \|h(x)\|^2 + \delta \frac{k_i}{i_d^{op} \omega^d} \|h(x)\| \quad (73)$$

$$= -k_d \gamma_F (i_d - i_d^{op})^2 - (1 - \theta) \lambda_{\min} \|h(x)\|^2 - \theta \lambda_{\min} \|h(x)\|^2 + \delta \frac{k_i}{i_d^{op} \omega^d} \|h(x)\| \quad (74)$$

$$\leq -k_d \gamma_F (i_d - i_d^{op})^2 - (1 - \theta) \lambda_{\min} \|h(x)\|^2, \quad \forall \|h(x)\| \geq \delta \frac{k_i}{i_d^{op} \omega^d \theta \lambda_{\min}} \quad (75)$$

This result concludes that the system will remain bounded by

$$\|h(x)\| \leq \delta \frac{k_i}{i_d^{op} \omega^d \theta \lambda_{\min}}. \quad (76)$$

Notice that small values of k_i reduce the error in i_F , which it turns in a better reactive power compensation and also in a reduction of the δ bound.

In order to show that $\dot{H}_{dz} \leq 0$, note that the SIDA-PBC design implies $(\partial_x H_d)^T F_d \partial_x H_d \leq 0$, from where we can conclude that the system is stable if the following condition holds

$$k_i \left| \frac{\gamma_F (i_F - z) (Q_s - Q_s^d)}{i_d^{op} \omega^d} \right| \leq |(\partial_x H_d)^T F_d \partial_x H_d|. \quad (77)$$

At this point we recover the time-scale argument, where for values of i_F close to z (*i.e.*, i_F^d), the range of k_i can be enlarged.

Finally, computing the right hand side of (77), it is possible to provide a simplest, but also more restrictive, constraint. Using that $-k_d \gamma_F (i_d - i_d^{op})^2 \leq 0$ and $-B_r \gamma_\omega (\omega - \omega^d)^2 \leq 0$, a stability condition on the error of Q_s can be found:

$$\left| Q_s - Q_s^d \right| \leq \frac{n_p M \gamma_F}{k_i} \left| i_d^{op} \omega^d i_q \left(\frac{1}{4} n_p M \gamma_F^2 i_q (i_F - z) - \gamma_q (i_q - i_q^*) \right) \right|. \quad (78)$$

Note that this equation also provides a bound for the initial conditions of the system such that our stability argument holds rigorously.

5 Simulations

In this section we present some simulations using the designed controller in Section 4. The WRSM parameters are: $L_s = 1\text{mH}$, $R_s = 0.0303\Omega$, $M = 1.5\text{mH}$, $L_F = 8.3\text{mH}$, $R_F = 0.0539\Omega$, $n_p = 2$, $J_m = 0.01525\text{kg}\cdot\text{m}^2$, $B_r = 0.05\text{N}\cdot\text{m}\cdot\text{s}$ and $\tau_L = 1\text{N}\cdot\text{m}$. The control parameters are selected as: $k_d = 50$, $k_F = 1$, $k_\omega = 0.05$ and $k_i = 200$, and the desired reactive power is, in all cases, set to zero, $Q_s^d = 0$.

The first numerical experiment is performed increasing the desired speed from $\omega^d = 200\text{rad}\cdot\text{s}^{-1}$ to $\omega^d = 250\text{rad}\cdot\text{s}^{-1}$ at $t = 0.01\text{s}$. For these values, the optimal value of i_d , computed in (37) changes from $i_d^{op} = 5.32\text{A}$ to $i_d^{op} = 5.88\text{A}$. Figure 4 shows that the system is perfectly regulated under changes of the desired outputs.

Figure 5 shows the results of a second test. In this case the external torque is suddenly changed at $t = 0.01$ from $\tau_L = -1\text{N}\cdot\text{m}$ to $\tau_L = 1.5\text{N}\cdot\text{m}$. Now the optimal value of i_d goes from $i_d^{op} = 5.32\text{A}$ to $i_d^{op} = 3.5\text{A}$. Note that this torque change also involves a change of the power sign in the stator side, and the WRSM is now generating electric energy. Figure 6 shows the behaviour of the stator active power and the bidirectional ability of the proposed controller.

6 Conclusions

The SIDA-PBC technique has been applied to control a wound rotor synchronous machine for a motor drive application. The SIDA-PBC matching equation has been solved using the algebraic approach and the desired robustness of the resulting controller has been taken into account. The obtained inner-loop controller has a simpler architecture than the standard one, is globally asymptotically stable, assures stability for a large range of control gain values, and works for either positive or negative load torque, thus displaying bidirectional power behavior. The stability of the inner-loop has been proved rigorously using passive port-Hamiltonian based techniques. In the stability analysis the damping coefficient (which is present in all real machines) plays a fundamental role to ensure convergence to the equilibrium point. Also, an additional outer loop that takes into account the power factor regulation has been introduced and the stability of the complete controller has been discussed and is proved for a region of the state space. The presented method also allows to decouple the outputs, improving the robustness and facilitating the gain tuning.

A power analysis, which allows to estimate the optimal value of i_d in order to minimize losses is also presented. This off-line computation, which depends on the machine parameters and the mechanical torque, is used to reduce the machine losses.

Future research includes a dynamical extension keeping the Hamiltonian structure to improve the robustness (basically on the electrical parameters R_s , L_s , M , and R_F) and the performance. This can be easily done for the i_d and i_F currents (due to the fact that they are passive outputs), but a more complicated task is to design a dynamical extension for the speed part. Experimental validation with a real plant using the control law designed in this paper will be also considered in the future.

7 Acknowledgments

Arnau Dòria-Cerezo and Carles Batlle were partially supported by the Spanish government research projects DPI2007-62582 and DPI2008-01408, respectively, while Gerardo Espinosa-Pérez was supported by DGAPA-UNAM (IN112908) and CONACYT (51050).

References

- [1] Rossi C, Casadei D, Pilati A, Marano M. Wound Rotor Salient Pole Synchronous Machine Drive for Electric Traction. In: Proc. IEEE Industry Applications Conference; 2006.
- [2] Schaefer RC. Excitation Control of the Synchronous Motor. IEEE Trans on Industry Applications. 1999;35(3):694–702.
- [3] Leonhard W. Control of electric drives. Springer; 1995.
- [4] Senesky MK, Tsao P, Sanders SR. Simplified modelling and control of a synchronous machine with variable-speed six-step drive. In: Proc. IEEE Applied Power Electronics Conference and Exposition; 2004.
- [5] Ho E, Sen PC. High-Performance Decoupling Control Techniques for Various Rotating Field Machines. IEEE Trans on Industrial Electronics. 1995;42(1):40–49.
- [6] Magri AE, Giri F, Abouloifa A, Haloua M. Nonlinear Control of Wound-Rotor Synchronous-Motor. In: Proc. IEEE Int. Conf. Control Applications; 2006. p. 3110–3115.
- [7] Marino R, Tomei P, Verrelli CM. Adaptive Field-oriented Control of Synchronous Motors with Damping Windings. European Journal of Control. 2008;14(3):177–200.
- [8] Zeraoulia M, Benbouzid MEH, Diallo D. Electric Motor Drive Selection Issues for HEV Propulsion Systems: A Comparative Study. IEEE Trans on Vehicular Technology. 2006;55(6):1756–1764.
- [9] Nicklasson PJ, Ortega R, Espinosa-Pérez G. Passivity-based control of a class of Blondel-Park transformable electric machines. IEEE Trans on Automatic Control. 1997;42(5):629–647.

- [10] Espinosa-Pérez G, Godoy-Alcantar M, Guerrero-Ramírez G. Passivity-based control of synchronous generators. In: Proc. IEEE Int. Symposium on Industrial Electronics; 1997.
- [11] Guo Y, Xi Z, Cheng D. Speed regulation of permanent magnet synchronous motor via feedback dissipative Hamiltonian realisation. IET Control Theory Appl. 2007;1(1):281–290.
- [12] Ortega R, van der Schaft A, Maschke B, Escobar G. Interconnection and damping assignment passivity-based control of port-controlled Hamiltonian systems. Automatica. 2002;38(4):585–596.
- [13] Rodriguez H, Ortega R. Interconnection and damping assignment control of electromechanical systems. Int J of Robust and Nonlinear Control. 2003;13:1095–1111.
- [14] Batlle C, Dòria-Cerezo A, Ortega R. Power Flow Control of a Doubly-Fed Induction Machine Coupled to a Flywheel. European Journal of Control. 2005;11(3):209–221.
- [15] Petrovic V, Ortega R, Stankovic AM. Interconnection and damping assignment approach to control of PM synchronous motors. IEEE Trans on Control Systems Technology. 2001;9(6):811–820.
- [16] Batlle C, Dòria-Cerezo A, Espinosa G, Ortega R. Simultaneous Interconnection and Damping Assignment Passivity-Based Control: The Induction Machine Case Study. Int Journal of Control. 2009;82(2):241–255.
- [17] Dòria-Cerezo A. Modeling, simulation and control of a doubly-fed induction machine controlled by a back-to-back converter. Universitat Politècnica de Catalunya; 2006. Available on-line: <http://www.tdcat.cesca.es/TDX-1212106-110114/index.html>.
- [18] Ortega R, van der Schaft A, Mareels I, Maschke B. Putting energy back in control. IEEE Control Syst Mag. 2001;p. 18–33.
- [19] Dalsmo M, van der Schaft A. On representations and integrability of mathematical structures in energy-conserving physical systems. SIAM J Control Optim. 1998;37:54–91.
- [20] van der Schaft A, Maschke B. Port controlled Hamiltonian systems: modeling origins and system theoretic properties. In: Proc. 2nd IFAC Symp. on Nonlinear Control Systems Design (NOLCOS'92); 1992. p. 282–288.

- [21] Fujimoto K, Sugie T. Canonical transformations and stabilization of generalized Hamiltonian systems. *Systems & Control Letters*. 2001;42(3):217–227.
- [22] Ortega R, Garcia-Canseco E. Interconnection and Damping Assignment Passivity-Based Control: A Survey. *European Journal of Control*. 2004;10(5):432–450.
- [23] Krause PC, Wasynczuk O, Sudhoff SD. *Analysis of Electric Machinery and Drive Systems*. John Wiley & Sons Inc.; 2002.
- [24] Chiasson J. *Modeling and High Performance Control of Electric Machines*. John Wiley & Sons Inc.; 2005.
- [25] van der Schaft A. *L_2 gain and passivity techniques in nonlinear control*. Springer; 2000.
- [26] Kugi A. *Non-linear control based on physical models*. Springer; 2001.
- [27] Batlle C, Dòria-Cerezo A, Espinosa G. Simultaneous IDA-Passivity-based control of a Wound Rotor Synchronous Motor. In: *Proc. IEEE Conf. on Decision and Control*; 2008. p. 3187–3191.
- [28] Khalil H.K. *Nonlinear Systems*. Prentice Hall; 2002.

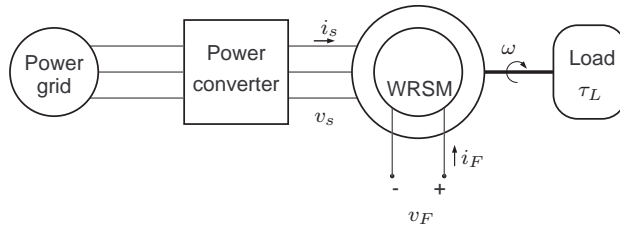


Figure 1: Scheme of a wound rotor synchronous machine acting as a motor.

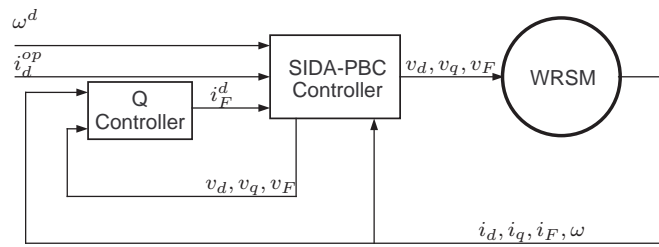


Figure 2: Proposed control scheme.

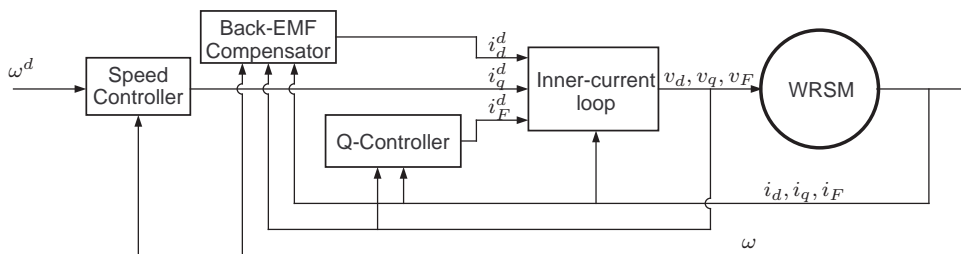


Figure 3: Classical control scheme.

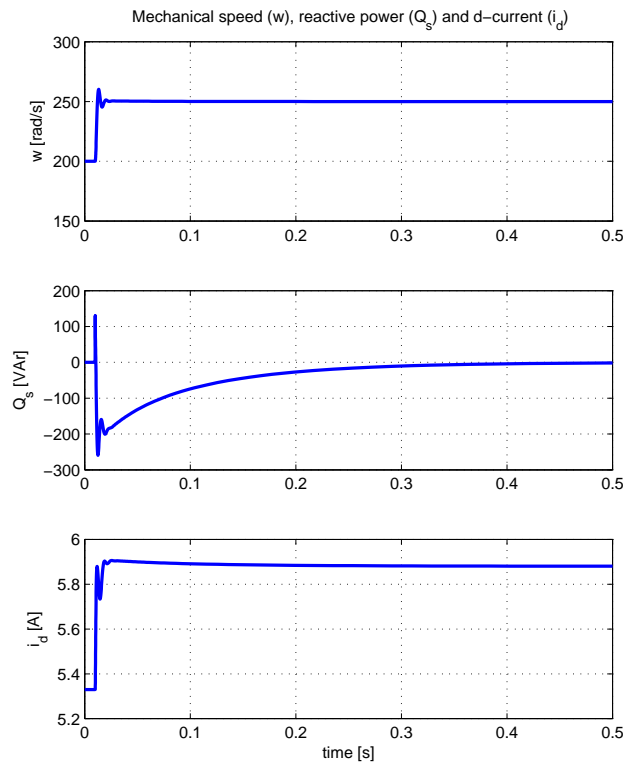


Figure 4: Simulation results: Mechanical speed, reactive power and i_d current, under a change of the speed reference.

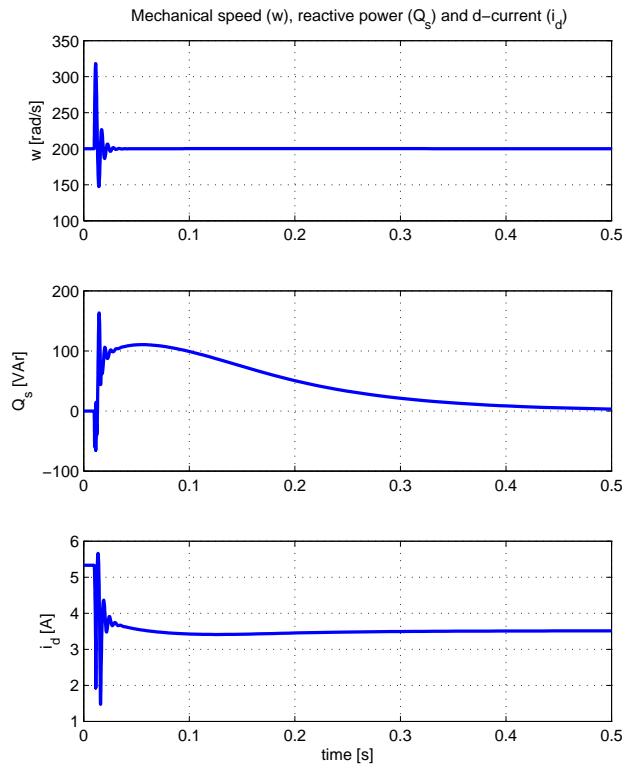


Figure 5: Simulation results: Mechanical speed, reactive power and i_d current, under a change of the external torque, from dissipative to regenerative.

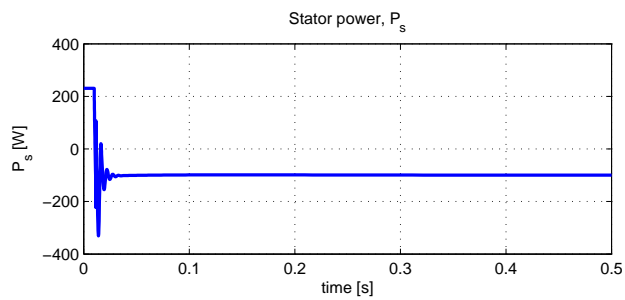


Figure 6: Simulation results: Stator active power P_s , under a change of the external torque, from dissipative to regenerative. As τ_L reverses sign, while at the same time keeping the regulated value of ω , the sign of P_s also changes.